Metabolic alterations in different developmental stages of Pilocarpus microphyllus

Abreu, I.N.; Choi, Y.H.; Sawaya, A.C.H.F.; Eberlin, M.N.; Mazzafera, P.; Verpoorte, R.

Metabolic Alterations in Different Developmental Stages of *Pilocarpus microphyllus*

Authors Ilka N. Abreu[1,2], Young H. Choi[4], Alexandra C. H. F. Sawaya[2,3], Marcos N. Eberlin[3], Paulo Mazzafera[2], Robert Verpoorte[4]

Affiliations
[1] Plant Product and Food Quality Department, Scottish Crop Research Institute, Invergowrie Dundee, United Kingdom
[2] Department of Plant Physiology, Institute of Biology, University Estadual of Campinas, Campinas, SP, Brazil
[3] Thomson Mass Spectrometry Lab, Institute of Chemistry, University Estadual of Campinas, Campinas, SP, Brazil
[4] Section of Metabolomics, Division of Pharmacognosy, Leiden University, IBL, Leiden, The Netherlands

Key words
- jaborandi
- *Pilocarpus microphyllus*
- Rutaceae
- metabolic change
- NMR
- MS
- metabolomics

Abstract

Pilocarpine is an imidazole alkaloid that has been used for more than a century in glaucoma treatment. It is present in several species of the *Pilocarpus* genus (jaborandi), with its highest concentrations in *P. microphyllus*. In addition to pilocarpine, pilosine – an imidazole alkaloid without pharmacological use – is produced in high concentrations in mature plants. A metabolomic study was carried out on juvenile and mature plants to obtain information about pilocarpine metabolism at different developmental stages. Methanol-water and alkaloid extracts were analyzed by ^{1}H NMR and ESI-MS. Metabolic profiles from both techniques showed clear differences between various developmental stages. Intense signals in the aromatic region of the ^{1}H NMR spectrum and ions from pilosine and related alkaloids by ESI/MS were found only in extracts from mature plant. Two new imidazole alkaloids were identified by MS^n. Our results suggest that pilosine is produced exclusively in mature developmental stage, and juvenile plant material seems to be appropriate for further studies on pilocarpine biosynthesis.

Introduction

The genus *Pilocarpus* (Rutaceae) comprises native species from the north and northeast of Brazil, which are popularly known as jaborandi. *P. microphyllus* is economically the most important representative of jaborandi because it contains high concentrations of the imidazole alkaloid, pilocarpine, which is used to treat glaucoma as a stimulant of lachrymal and sweat glands and in the control of xerostomia [1]. In addition to pilocarpine, other imidazole alkaloids such as 3-nor-8 (11)-dihydropilocarpine, anhydropilosine, pilosine, and pilosinine have also been found in jaborandi leaf extracts [2–5]. However, of all these imidazole alkaloids produced in *P. microphyllus,* only pilocarpine has pharmaceutical applications. For this reason, deeper insight into the biosynthesis and metabolic regulation of imidazole alkaloids could potentially allow manipulation or metabolic engineering favouring pilocarpine synthesis over the biosynthesis of other alkaloids. We previously reported on pilocarpine regulation under stress conditions [6], molecular diversity in jaborandi [7], characterization of the imidazole alkaloid profile in different seasons and identification of novel alkaloids [8], selection of cell suspensions lines for biosynthesis studies [9], and cell lines producing only pilocarpine [10].

A preliminary study using jaborandi from different developmental stages showed that mature plants produce similar amounts of pilosine and pilocarpine, but during juvenile stages only pilocarpine was found. However, as yet a detailed study on developmental aspects of imidazole alkaloid biosynthesis in *P. microphyllus* is not available.

Since plants are sessile, they have evolved specific strategies to cope with environmental changes. Generally, these adaptations to stress involve significant changes in metabolism [11]. Metabolic changes can also be a predetermined and essential part of plant development [12–15].

Detection of metabolic perturbation was traditionally a laborious undertaking but the advent of more sensitive analytical technologies, in particular time-of-flight-MS, has meant that metabolite changes can be reported effectively and reproducibly. The most commonly employed techniques are ^{1}H NMR, GC-MS, and direct infusion electrospray ionization mass spectrometry [16], and these are utilized to detect changes in the patterns of metabolites related to developmental, genetic, or environmental changes. Although ^{1}H

received January 26, 2010
revised June 11, 2010
accepted August 5, 2010

Bibliography
DOI http://dx.doi.org/10.1055/s-0030-1250314
Published online September 15, 2010
Planta Med 2011; 77: 293–300

ISSN 0032-0943

Correspondence
Dr. Ilka Nacif de Abreu
Plant Product and Food Quality Department
Scottish Crop Research Institute
Invergowrie Dundee DD2 5DA
United Kingdom
Phone: + 44 13 82 56 27 31 31 14
Fax: + 44 13 82 56 85 03
ilka.abreu@scri.ac.uk

NMR has relatively low sensitivity compared to mass spectrometry (MS), it has the advantage of allowing the detection of diverse groups of plant metabolites [12]. The characterization and quantification of predominant metabolites with the help of metabolomic profiles and subsequent multivariate data analysis permit the identification of specific biosynthetic pathways in plant material [17].

Multivariate statistical analyses have been shown to provide interpretable models for large complex data sets and have become a standard part of global metabolite analytical techniques [18]. One of the supervised multivariate data analysis methods for metabolomics is Orthogonal Projection to Latent Structures – OPLS [19], where the systematic variation in data can be separated into a predictive (variation of interest) and an orthogonal component [20].

Here, we carried out a metabolomic study on jaborandi plants during different stages of their development, using ^{1}H NMR and ESI-MS associated to multivariate analysis in order to obtain information regarding the production of imidazole alkaloids in *P. microphyllus*.

Material and Methods

Plant material

Plants of *P. microphyllus*, obtained from germinated seeds donated by Merck, were cultivated under standard greenhouse conditions. The plants were grown in 5 L plastic pots containing a mixture of soil/sand (2 : 1, v/v). Three plants at juvenile and mature (vegetative and flowering) stages were selected for the analyses. The juvenile plants were divided in seven parts (**Fig. 1 C**), from the apex to the base and classified as follows, youngest (VVY), very young (VY), young (apical and basal – YA, YB), intermediate (apical and basal – IA, IB), old leaves (O), stem (S), and root (R). Mature plants were analyzed in the vegetative and flowering stages (only the intermediate leaves). A voucher specimen was deposited in the herbarium of the Biology Institute (University of Campinas – Brazil) with reference number 150 316 (Feb 2009).

Alkaloids extractions

Fresh material (700 mg) was crushed in a mortar with 5–6 drops of 10% NH_4OH and transferred to plastic tubes. After 15 min, 5 mL of chloroform was added, and the mixture vigorously shaken and then centrifuged to recover the organic solvent. This was repeated three times. The organic fractions were pooled and twice extracted with 2 mL of 2% H_2SO_4. The acid fractions were pooled and the pH brought to 12 with NH_4OH. After two extractions with 2 mL chloroform, the organic fractions were pooled and dried in a Speed-Vac. High performance liquid chromatography (HPLC) buffer with the pH adjusted to 5.0 was added to the dried extract and retained for analysis.

Alkaloids quantifications

The chromatography was performed on a HPLC (Shimadzu) system, coupled to a diode array detector (Shimadzu). Twenty µL of alkaloid extract were injected onto a Supelcosil LC18 column (250 mm × 4.6 mm, 5 mm; Supelco) using as solvent a buffer containing 1.3% H_3PO_4, 0.3% triethylamine, and 12% methanol (pH 3.0), at a flow rate of 1 mL·min^{-1}. The diode array detector was set to operate from 190 to 340 nm, and pilocarpine and pilosine were determined at 212 nm, as previously described [21].

NMR extractions

After collection, the materials were immediately frozen in liquid nitrogen and kept at − 80 °C. One gram (powder) was transferred to a centrifuge tube and extracted as described previously by Choi et al. [15]: fifteen milliliters of 50% water-methanol mixture and 15 mL of chloroform were added to the tube, followed by vortexing for 30 s and sonication for 1 min. The sample was then centrifuged at 3000 rpm for 20 min. The aqueous and organic fractions were collected separately. Each fraction was placed in a round-bottom evaporation flask and dried in a rotary vacuum evaporator. The dried aqueous fractions were dissolved in 0.8 mL of deuterated solvent, 50% methanol-d_4 in D_2O (KH_2PO_4 buffer, pH 6.0) containing 0.05% TMSP (trimethylsilylpropionic acid sodium salt, w/w) for the NMR analysis.

NMR measurements

^{1}H NMR, J resolved, HMBC, and COSY spectra were recorded at 25 °C on a 500 MHz Bruker DMX-500 spectrometer (Bruker) operating at a proton NMR frequency of 500.13 MHz. Each ^{1}H NMR spectrum consisted of 128 scans requiring a 10-min and 26-s total acquisition time with the following parameters: 0.16 Hz/point, pulse width (PW) = 30° (11.3 µs), and relaxation delay (RD) = 1.5 s. A presaturation sequence was used to suppress the residual H_2O signal with low power selective irradiation at the H_2O frequency during the recycle delay. Free induction decays (FIDs) were Fourier-transformed with an exponential line broadening corresponding 0.3 Hz. The resulting spectra were manually phased and baseline-corrected and calibrated to TMSP at 0.0 ppm, using XWIN NMR (version 3.5; Bruker). 2D J-resolved NMR spectra were acquired using 8 scans per 128 increments for F1 and 8K for F2 using spectral widths of 5000 Hz in F2 (chemical-shift axis) and 66 Hz in F1 (spin-spin coupling constant axis). A 1.5 s relaxation delay was employed, giving a total acquisition time of 56 min. Data sets were zero-filled to 512 points in F1 and both dimensions were multiplied by sine-bell functions (SSB = 0) prior to double complex FT. ^{1}H-^{1}H correlated spectroscopy (COSY) spectra were recorded on a 500 MHz Bruker DMX-500 spectrometer (Bruker). The COSY spectra were acquired with a 1.0 s relaxation delay and 6361 Hz spectral width in both dimensions. The window function for COSY spectra was sine-bell (SSB = 0).

MS measurements

10 µL of the alkaloid extracts were dissolved in 1 mL of water and acetonitrile (1 : 1, v/v, containing 0.1% of formic acid) for mass spectrometric analysis as previously described [22]. The tandem mass spectra were acquired on an Applied Biosystems Q-trap mass spectrometer comprising a triple quadrupole and a linear ion trap, over a mass range of *m/z* 50–400. The operational parameters used for acquiring the ESI mass spectra were: capillary 5000 V, temperature 200 °C, declustering potential 70 V, and entrance potential 6 V. For the ESI-MS^2 and ESI-MS^3 experiments the above conditions were maintained and the collision energy was optimized in the range between 15 and 30 V for each protonated alkaloid or product ion analyzed.

Data analysis

The ^{1}H NMR spectra were automatically reduced to ASCII files using AMIX (v. 3.8; Bruker Biospin). Before, spectral intensities were scaled to total intensity and reduced to integrated regions of equal width (0.04 ppm) corresponding to the region of δ 0.4–10.00. The region of δ 4.70–5.10 and 3.28–3.34 was excluded

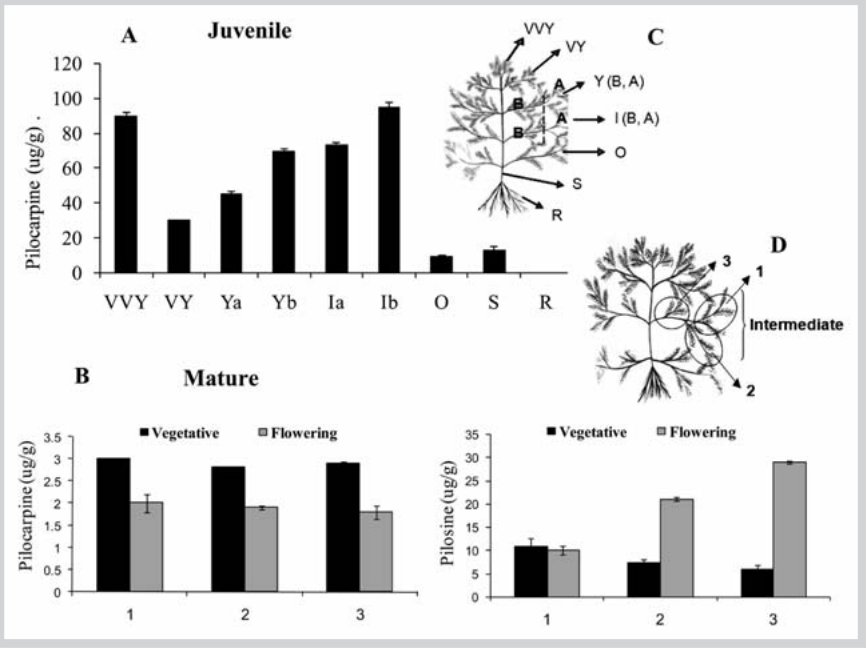

Fig. 1 Pilocarpine and pilosine levels (µg/g FW) at different developmental stages of *P. microphyllus*. **A** – **juvenile**: youngest (VVY), very young (VY), young (apical and basal – YA, YB), intermediate (apical and basal – IA, IB), old leaves (O), stem (S), and root (R); **B – mature:** intermediate leaves (basal, middle and apical – 1, 2, and 3) of plants in vegetative and flowering developmental stage. **C** and **D** – illustration of vegetative material analyzed from juvenile and mature plants.

from the analysis because of the residual signal of water and methanol-*d4*. Bucketing was performed by AMIX software (Bruker) with scaling on total intensity (autoscaling). Multivariate analysis was performed with the help of SIMCA-11.5 (Umetrics) using either unsupervised principal component analysis (PCA) or supervised orthogonal partial least square analysis (OPLS) [23]. OPLS is a supervised analysis tool that has been used to reveal differences in the metabolite profiles masked by PCA using all data points [19]. OPLS allows one to focus on variance due to developmental differences alone while minimizing other biological or analytical variables. For both PCA and OPLS, spectral regions were X-matrix. All X-variables were pareto scaled to minimize the influence of baseline deviations and noise. For OPLS, class difference (juvenile versus mature) was the Y-matrix. The spectral regions of juvenile plant samples (**Fig. 1C**) were the X-matrix for PCA analysis. The quality of each model was determined by the goodness of R^2 and the prediction parameter based on the cross-validation (Q^2).

General

Pilocarpine (98% purity) was purchased from Sigma, and pilosine (90% purity) was a gift from Merck Laboratories. Solvents used for leaf extraction were of analytical grade (Merck). NMR spectra were recorded on a Bruker DMX-500 spectrometer (Bruker) using CD_3OD (99.96%) and D_2O (99.0%) purchased from Cambridge Isotope Laboratories Inc.

Results and Discussion

The quantification of pilocarpine and pilosine by HPLC-DAD is shown in **Fig. 1**. The pilocarpine levels in juvenile plants were three times higher than in mature plants. Pilosine was absent in juvenile plants (**Fig. 1A**), however present in higher amounts (ten times more) than pilocarpine in mature plants. The flowering stage seems to be important for pilosine production, although the pilocarpine levels were higher during the vegetative stage of mature plants (**Fig. 1B**).

In order to obtain information that could help to characterize the developmental stages in *P. microphyllus*, a metabolomic analysis was performed by NMR. The methanol-water extracts of several parts of juvenile plants and the intermediate leaves of mature plants (vegetative and flowering stages) were analyzed by ^1H NMR and exhibited similar profiles to the ones shown in **Fig. 2A**. The inevitable problem of overlapping signals (which could be an obstacle for metabolite identification) was solved by acquiring ^1H-^1H COSY and 2D J-resolved NMR spectra (**Fig. 2B** and **C**). The combination of the results from the 2D experiments and the library of NMR spectra of several standards in the Division of Pharmacognosy (Institute of Biology, Leiden University) allowed us to identify some of the contrasting signals, thereby facilitating the assignment of the spectra (**Table 1**).

The amino and organic acids, and sugar region (δ 0.8–4.0) showed signals characteristic of threonine, valine, leucine, isoleucine, alanine, asparagine, glutamine, glycine, choline, inositol, acetate, malate, succinate, and fumarate. The sugars glucose and sucrose were found at δ 4.58, 5.18 and 5.40, respectively. Strong signal intensity in the aromatic region (δ 6.0–8.5) was identified as flavonoids, tyrosine, histidine, and signals related to the alkaloids pilosine and anhydropilosine. However, several other signals in this region could not be identified. The signals related to imidazole rings were found at δ 8.53 and 7.18 and lactone rings at δ 4.44 and 4.18, which were confirmed by comparison with pilocarpine and pilosine standards.

The principal component analyses (PCA) were performed using data from juvenile and mature plants (**Fig. 3**), which showed a model ($R^2X = 0.836$; $Q^2 = 0.653$) with 6 significant components. The different parts of juvenile plants clustered into a distinct group compared to the adult plants (**Fig. 3A**). The first component axis (PC1) separated top leaves and stem (VVY and S) from the bottom leaves (O). PC2 shows the discrimination of roots (R) from the other samples and also mature plants in vegetative or flowering developmental stage. Because the loading plot of PC2 included metabolites related to the very young and young leaves (VY and YA, B) from juvenile plants and also samples from mature

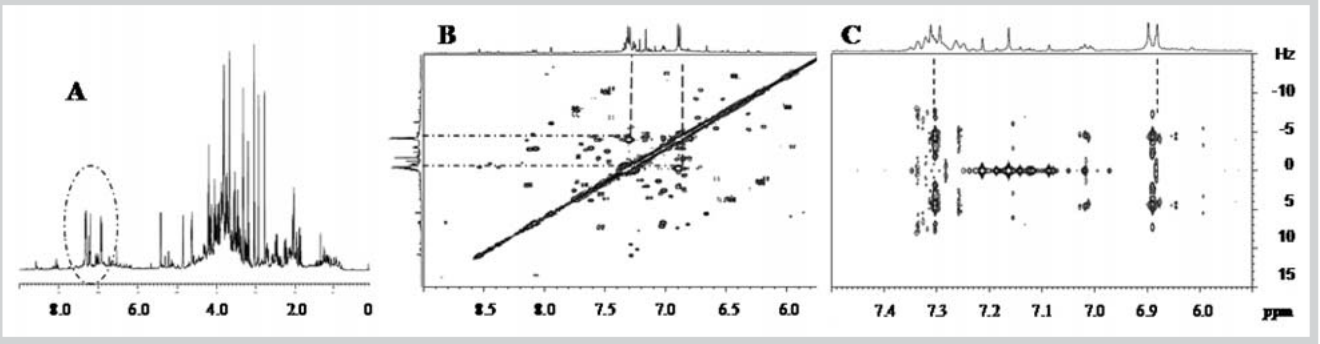

Fig. 2 ^{1}H NMR (**A**), ^{1}H-^{1}H COSY (**B**), and J-resolved (**C**) spectra of methanol-water extract of *P. microphyllus* mature intermediate leaves. Dashed lines show an example of tyrosine identification, displaying signals from H (3, 5) and H (2, 6) of aromatic ring.

Table 1 ^{1}H chemical shift and coupling constants of metabolites of *P. microphyllus* leaves detected from 1 and 2 D NMR spectra (CD_3OD-KH_2PO_4 in D_2O).

Compound	Chemical shift (δ) and Coupling constants (Hz)
Treonine	1.32 (d, J = 6.6, H-4)
Valine	1.17 (d, J = 6.8, H-5), 1.19 (d, J = 6.8, H-4)
Leucine	3.60 (d, J = 1.4, CH_2)
Isoleucine	3.52 (d, J = 2.2, CH_2)
Alanine	1.49 (d, J = 7.2, H-3)
Asparagine	2.80 (dd, J = 16.9, J = 4.3, H-3), 2.41 (dd, J = 16.9, J = 2.96, H-3)
Glutamine	2.10 (m, H-3), 2.5 (td, J = 16.2, 7.6, H-4)
Choline	3.21 (s)
Inositol	3.45 (dd, J = 9.9, H-1 and 3)
Glycine	3.58 (s)
β glucose	4.58 (d, J = 7.9, H-1)
α glucose	5.18 (d, J = 3.8, H-1)
Sucrose	5.40 (d, 3.9, H-1), 4.17 (d, J = 8.5, H-1)
Histidine	8.75 (s), 7.4 (s)
Acetate	1.88 (s)
Malate	2.6 (dd, H-3, J = 4.7, 16.6), 2.42 (dd, H-3, J = 6.6, 16.6)
Succinate	2.53 (s)
Fumarate	6.40 (s)
Tyrosine	6.81 (d, J = 8.6, H-3,5), 7.22 (d, J = 8.6, H-2,6)
Pilocarpine	8.53 (s, H-2), 7.18 (s, H-5), 4.18 (dd, J = 2.2, J = 1.2, H-8), 4.44 (dd, J = 3.0, J = 1.2, H-8), 2.21 (dd, J = 2.2, J = 4.4, H-6), 2.42 (dd, J = 2.2, J = 4.4, H-6), 3.70 (s, N-CH_3)
Pilosine	6.52 (s, H-5), 2.84 (m, H-7), 4.4 (dd, J = 2.2, J = 1.3, H-8), 4.0 (dd, J = 3.0, J = 1.3, H-8), 2.76 (m, H-11), 3.72 (s, N-CH_3)
Anhydropilosine	6.19 (s, H-12)
Quercetin-3-glucoside	6.22 (d, J = 2.3, H-6), 6.39 (d, J = 2.3, H-8), 6.80 (d, J = 8.4, H-3′,5′), 8.06 (dd, J = 8.4, 2.0, H-2′,6′), 5.32 (d, J = 7.6)
Unkown flavonoid	CH_3Ram- 1.18 (d, J = 6.1), O-CH_3 – 3.85 (s), 6.9 (d, J = 5, H-3), 7.55 (dd, J = 10, J = 6.0, H-2), 8.05 (d, J = 5, H-6)

plants, its interpretation was difficult. So, the experiment was analyzed by a supervised multivariate analysis: OPLS.

The OPLS analysis was performed on the processed data, showing a model (R^2X = 0.396; R^2Y = 0.934; Q^2 = 0.868) with 2 significant components, where the predictive component could validate the model showing clear separation between mature and juvenile plants (**Fig. 3B**). The loading plot (**Fig. 3C**) revealed intense signals in the aromatic, sugar, and lactone ring region in mature plants (vegetative and flowering developmental stages). Tyrosine, sucrose, and β glucose were the most intense signals. By contrast, in juvenile plants high intensities for amino and organic acids signals were found. Since we have no knowledge of a previous study of *P. microphyllus* extracts analyzed by NMR, many signals in the aromatic region (which were significant in the analysis) could not be identified. Most of these signals could represent species-specific metabolites.

From **Fig. 3A**, the score plot showed clear distinction between different parts of juvenile plants. The data from mature plants was excluded, and a new PCA analysis (**Fig. 4**) was performed. From the model (R^2X = 0.848; Q^2 = 0.648) with 5 significant components, PC1 (**Fig. 4A**) revealed differences between top (very very young – VVY) and bottom leaves (O) and greater similarity between very young (VY), young (YA,B), and intermediate leaves (IA,B), see **Fig. 1C**. The comparison between the raw data of top and bottom leaves (**Fig. 4B**) shows intense signals at δ 3.84 in the bottom leaves and organic and amino acids region (δ 3.52, 3.21, 2.92, 2.36, and 2.21–1.8) on top leaves, referring to signals from isoleucine, choline, and acetate. Furthermore, PC2 (**Fig. 4A**) shows clear discrimination between root samples and the others, which seems to be related to the metabolites detected at δ 2.76–2.64 and δ 2.6–2.5 (**Fig. 4C**).

The analyses of methanol-water extracts by ^{1}H NMR, showed that the main differences between developmental stages in *P. microphyllus* plants was the high abundance of metabolites containing aromatic rings in mature plants (**Fig. 3**), which also affect the pilocarpine levels (**Fig. 1**). To understand how the developmental stages could affect the alkaloid profile, a thorough analysis of the alkaloid extracts from juvenile and mature plants was performed by ESI-MS in positive mode (**Fig. 5**).

The ESI(+)-MS of alkaloid extracts of mature leaves (**Fig. 5A**) demonstrated the presence of pilocarpine (1- *m/z* 209), as well as of ions with *m/z* 193, 227, 269, and 287 which are representative of 3-nor-8(11)–dihydropilocarpine, pilocarpic acid, anhydropilosine, and pilosine, respectively and ions with *m/z* 241, 259, 285, and 305, whose structures were described previously [8]. In the corresponding ESI-MS fingerprint of alkaloid extracts of juvenile plants (**Fig. 5B**) only the *m/z* 209 (pilocarpine) ion was present. The low intensity of this ion was probably due to the strong ionization of the ion of *m/z* 248, whose ESI(+)-MS^2 showed a different fragmentation pattern of imidazole alkaloids (data not shown). Taken together the ESI(+)-MS data confirm that juvenile plants solely accumulate pilocarpine, while pilosine along with other imidazole alkaloids are exclusively synthesized in mature plants (**Fig. 1**).

In order to search for new imidazole alkaloids, concentrated alkaloid extracts were analyzed. Two new ions *m/z* 301 and 319 were found only in the mature extracts (**Fig. 5C**). **Table 2** lists the ESI-MS^n fragments of the ions [**10** + H]$^+$ and [**11** + H]$^+$. Both com-

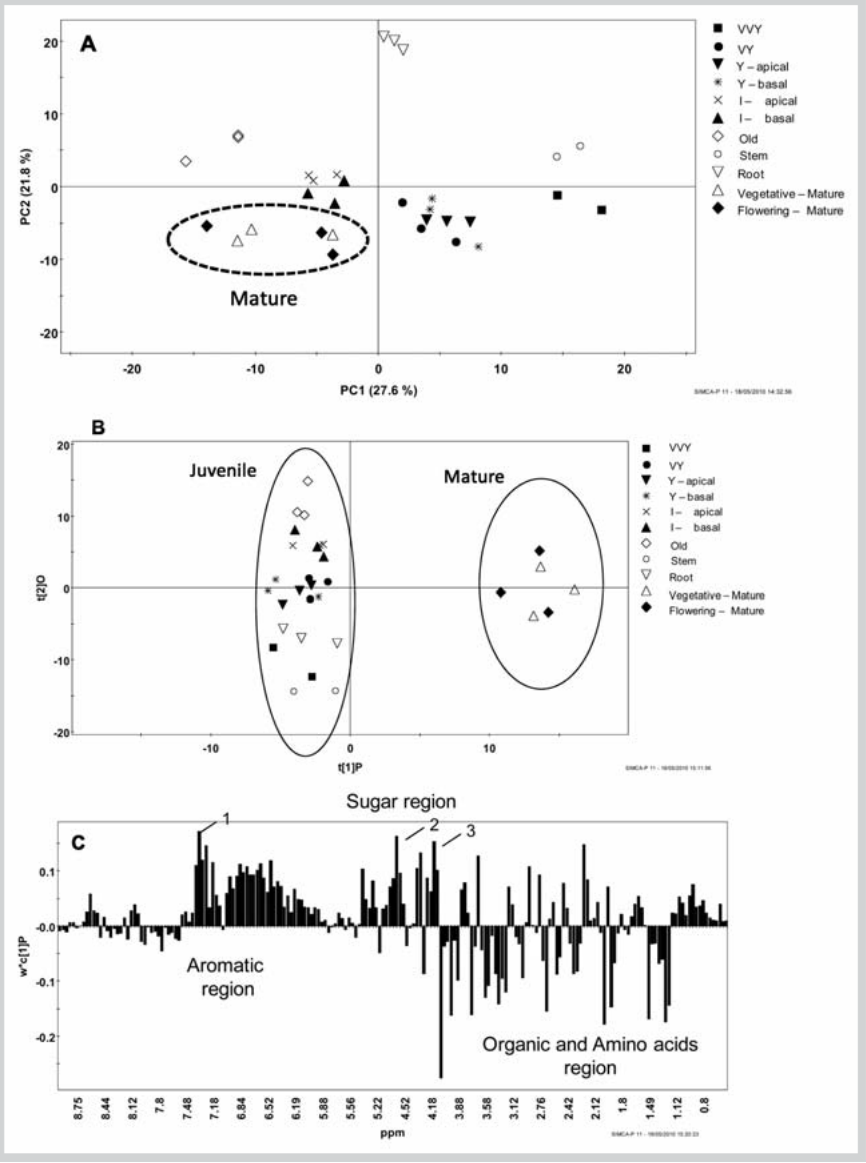

Fig. 3 Multivariate analysis of ^{1}H NMR data from *P. microphyllus* (in juvenile and mature developmental stages) extracts. **A** – Score plot of PCA analysis ($R^2X = 0.836$; $Q^2 = 0.653$); **B** – score plot of OPLS analysis ($R^2X = 0.396$; $R^2Y = 0.934$; $Q^2 = 0.868$); and **C** – loading plot of predictive component. Juvenile plants: leaves – VVY, VY, Y (apical, basal), I (apical, basal) and old leaves, stem, and root; mature plants: vegetative and flowering (**Fig. 1 C** and **D**); 1 – tyrosine (δ 7.22 – H-2 and 6), 2 – β glucose (δ 4.58), and 3 – lactone ring (δ 4.18, H-8).

Table 2 ESI tandem mass fragmentation of novel alkaloids (compounds **10** and **11**), present in the alkaloid extract of *P. microphyllus* leaves from mature plants in comparison with the fragmentation of anhydropilosine (compound **4**).

Compound	$[M - H]^+$ (m/z)	ESI (+)-MS^n experiment m/z (% base peak)
10	319	-MS^2 [319]: 319 (75), 301 (40), 269 (50), 223 (20), 181 (45), 163 (20), 121 (5), 95 (25)
	319	- MS^3 [319 → 301]: 301 (40), 269 (100), 223 (20), 163 (20)
	319	-MS^3 [319 → 269]: 269 (70), 251 (100), 185 (20), 95 (10)
11	301	-MS^2 [301]: 301 (100), 269 (35), 223 (15), 163 (20), 105 (5), 95 (5)
4	269	-MS^2 [269]: 269 (100), 251 (15), 223 (23), 121 (15), 95 (50)

pounds exhibited, as fragments, the diagnostic ion *m/z* 95 (1-methyl-5-imidazollymethyl cation), characteristic of imidazole alkaloids [8]. The collision-induced dissociation (CID) of *m/z* 319 resulted in the neutral loss of a water molecule (*m/z* 301); then, a further loss of O_2 to give the fragment *m/z* 269. This fragment was mass-selected and further fragmented via ESI-MS^3. When compared to the ESI-MS^2 of the *m/z* 269 ion found in the same extract, great similarity was observed indicating that both ions presented the same structure, which is compatible with anhydropilosine (**Fig. 5 D**). Relevant ions of fragments observed in both cases result from neutral losses of water (*m/z* 251) and CH_2O_2 (*m/z* 223) as well as of the diagnostic ion of *m/z* 95. Similarly, the fragment ion of *m/z* 301 was then mass-selected and further fragmented via ESI-MS^3. When compared to the ESI-MS^2 of the ion of *m/z* 301 found in the same extract, again significant similarity was observed indicating that both ions have the same structure, containing both the diagnostic ions of *m/z* 95 and *m/z* 105. The latter fragment was previously observed in the fragmentation of compounds **6** (*m/z* 241), **7** (*m/z* 259), and **8** (*m/z* 285) and is diagnostic of the C_6H_5-CO^+ cation [8].

Based on these fragmentation patterns, we propose that compound **10** (*m/z* 319) presents the basic structure of pilosine (which also fragments by losing water to form anhydropilosine (*m/z* 269) with two hydroxyls on the aromatic ring. The structure of compound **11** (*m/z* 301) is also similar, but the diagnostic fragment ion of *m/z* 105 indicates the presence of a ketone, similar to

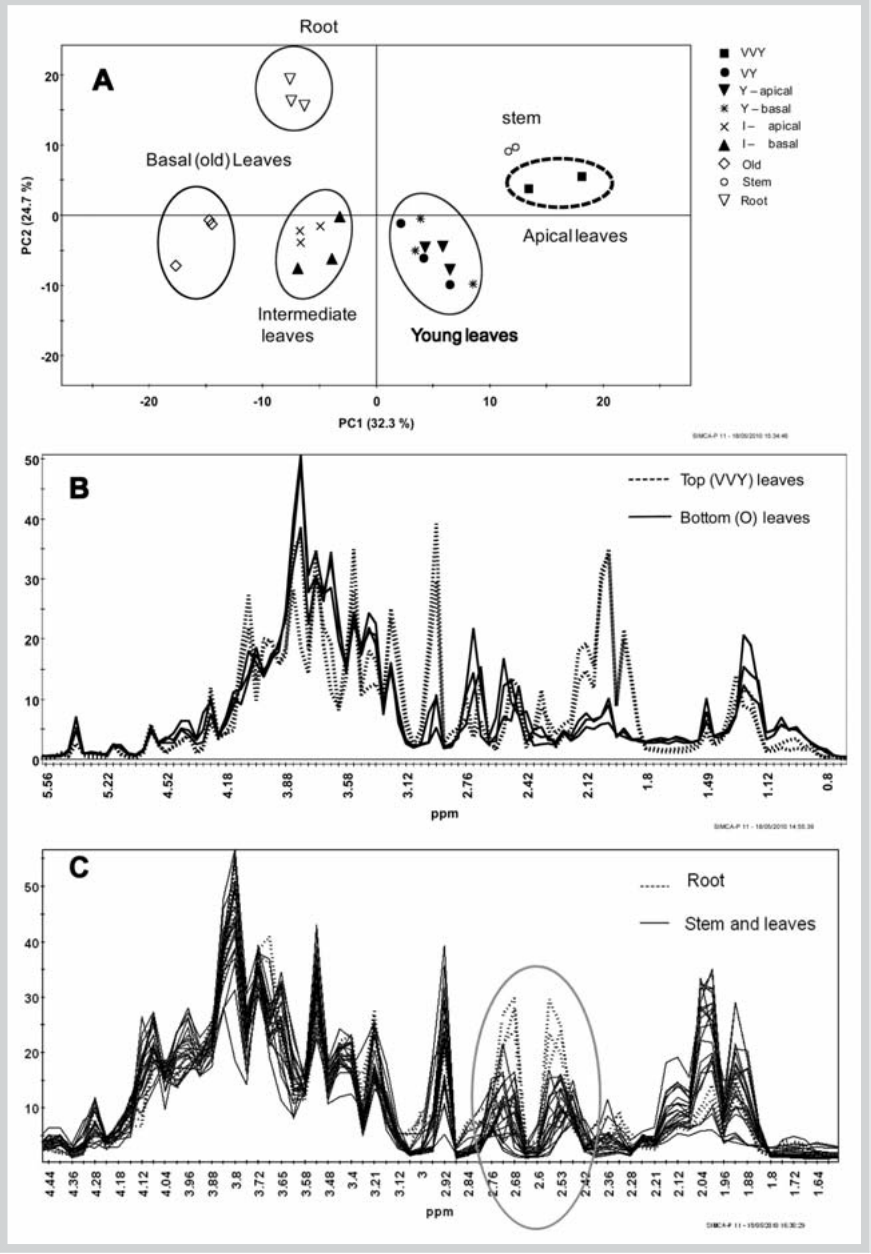

Fig. 4 PCA analysis of ^{1}H NMR spectral data from the extracts of different parts of *P. microphyllus* in juvenile stage ($R^2X = 0.848$, $Q^2 = 0.648$). Score plot (**A**) and comparison of raw data of selected samples: **B** – top (VVY) versus bottom (O) leaves; **C** – root versus leaves and stem.

compounds **6** (*m/z* 241) or **8** (*m/z* 285), as previously described in imidazole alkaloid synthesis [4].

In this study we have shown that NMR and MS are complementary techniques for the identification of different classes of metabolites in *P. microphyllus*. The aim of this work was to compare metabolomic data obtained from jaborandi plants at different developmental stages and to try to gain information on pilocarpine metabolism. To date, only a few alkaloids have been identified in jaborandi and there has been no previous study on their biosynthetic pathways. Pilocarpine is obtained commercially from jaborandi leaves, and pilosine is treated as a contaminant requiring additional purification steps. Therefore, since our results suggest that pilosine biosynthesis occurs only in mature plants, strategies to direct the metabolic flow exclusively to pilocarpine could be developed. In this regard, the juvenile material seems to be appropriate for such studies, as mainly pilocarpine is found in these tissues. However, there is still a significant lack of information on the biosynthesis of pilocarpine in plants, starting from the amino acid precursor. Recently, we validated the use of cell suspension cultures to study the control of pilocarpine biosynthesis [9] and selected lines producing only pilocarpine [10]. Metabolomic analysis by ^{1}H NMR and MS techniques using these lines may give support for futures studies on imidazole alkaloids biosynthesis in *P. microphyllus*.

Acknowledgements

Financial support was provided by the Fundação de Amparo à Pesquisa do Estado de São Paulo (FAPESP) and Coordenação de Apoio a Pesquisa (CAPES). The authors would like to thank D. Stewart, G. McDougall, U. Fischer, and P. White for reviewing the manuscript and providing helpful comments and suggestions.

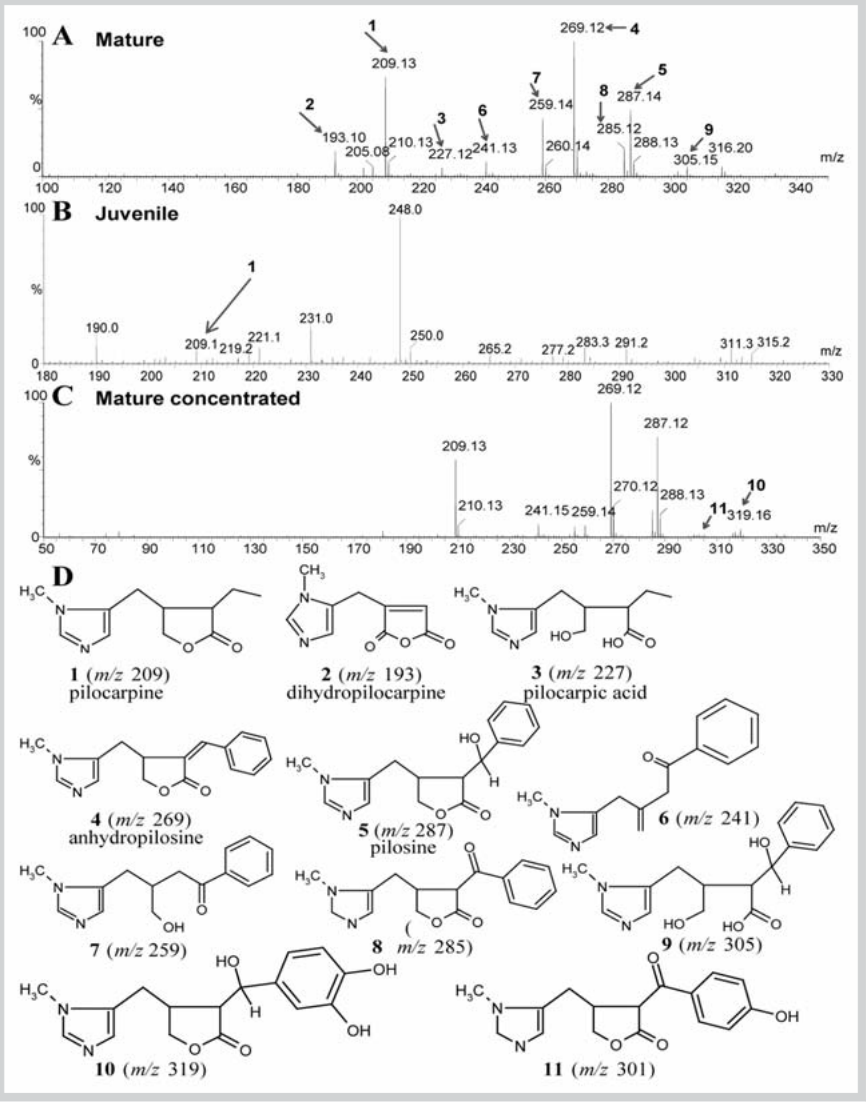

Fig. 5 ESI(+)-MS spectra of alkaloid extracts from intermediate leaves of **A** – mature and **B** – juvenile plants; **C** – concentrated alkaloid extract of mature plants and **D** – imidazole alkaloids of *P. microphyllus*.

References

1 *Pinheiro CUB.* Jaborandi (*Pilocarpus sp*, Rutaceae): a wild species and its rapid transformation into a crop. Econ Bot 1997; 51: 49–58

2 *Andrade-Neto M, Mendes PH, Silveira ER.* An imidazole alkaloid and other constituents from *Pilocarpus trachyllophus*. Phytochemistry 1996; 42: 885–887

3 *Voigtlander HW, Balsam G, Engelhardt M, Pohl L.* Epiisopiloturin, ein neues Pilocarpus-Alkaloid. Arch Pharm 1978; 311: 927–935

4 *Link H, Bernauer K.* Über die Synthese der *Pilocarpus*-Alkaloide Isopilosin und Pilocarpin, sowie die absolute Konfiguration des (+) Isopilosins. Helv Chim Acta 1972; 55: 1053–1062

5 *Link H, Bernauer K, Oberhans WE.* Configuration of *Pilocarpus* alkaloids. Helv Chim Acta 1974; 57: 2199–2200

6 *Abreu IN, Sawaya ACHF, Eberlin MN, Mazzafera P.* Production of pilocarpine in callus of jaborandi (*P. microphyllus* Stapf). In Vitro Cell Dev Biol Plant 2005; 41: 806–811

7 *Sandhu SS, Abreu IN, Colombo C, Mazzafera P.* Pilocarpine and molecular diversity in jaborandi. Sci Agric 2006; 63: 478–482

8 *Abreu IN, Mazzafera P, Zullo MAT, Eberlin MN, Sawaya ACHF.* Characterization of the variation of the imidazole alkaloid profile of *Pilocarpus microphyllus* in different seasons and parts of the plant by electrospray ionization mass spectrometry fingerprinting and identification of novel alkaloids by tandem mass spectrometry. Rapid Commun Mass Spectrom 2007; 21: 1205–1213

9 *Abreu IN, Andreazza NL, Sawaya ACHF, Eberlin MN, Mazzafera P.* Cell suspension as a tool to study the biosynthesis of pilocarpine in Jaborandi. Plant Biol 2007; 9: 793–799

10 *Andreazza NL, Abreu IN, Sawaya ACHF, Eberlin MN, Mazzafera P.* Production of imidazole alkaloids in cell cultures of jaborandi as affected by the medium pH. Biotechnol Lett 2009; 31: 607–614

11 *Weckwerth W.* Metabolomics in systems biology. Annu Rev Plant Biol 2003; 54: 669–689

12 *Jahangir M, Kim HK, Choi YH, Verpoorte R.* Metabolomic response of *Brassica rapa* submitted to pre-harvest bacterial contamination. Food Chem 2008; 107: 362–368

13 *Abdel-Farid BB, Kim HK, Choi YH, Verpoorte R.* Metabolic characterization of *Brassica rapa* leaves by NMR spectroscopy. J Agric Food Chem 2007; 55: 7936–7943

14 *Liang YS, Choi YH, Kim HK, Linthorst HJM, Verpoorte R.* Metabolomic analysis of methyl jasmonate treated *Brassica rapa* leaves by 2-dimensional NMR spectroscopy. Phytochemistry 2006; 67: 2503–2511

15 *Choi YH, Tapias EC, Kim HK, Lefeber AWM, Erkelens C, Verhoeven JTJ, Brzin J, Zel J, Verpoorte R.* Metabolic discrimination of *Catharanthus roseus* leaves infected by phytoplasma using ^{1}H NMR and multivariate data analysis. Plant Physiol 2004; 135: 2398–2410

16 *Castrillo JI, Hayes A, Mohammed S, Gaskell SJ, Oliver SG.* An optimized protocol for metabolome analysis in yeast using direct infusion electrospray mass spectrometry. Phytochemistry 2003; 62: 929–937

17 *Sumner LW, Mendes P, Dixon RA.* Plant metabolomics: large-scale phytochemistry in the funcional genomics era. Phytochemistry 2003; 62: 817–836

18 *Holmes E, Antti H.* Chemometric contributions to the evolution of metabonomics: mathematical solutions to characterising and interpreting complex biological NMR spectra. Analist 2002; 127: 1549–1557

19 *Trygg J, Wold S.* Orthogonal projections to latent structures (O-PLS). J Chemometrics 2002; 16: 119–128
20 *Pohjanen E, Thysell E, Lindberg J, Schuppe-Koistinen I, Moritz T, Jonsson P, Antti H.* Statistical multivariate metabolite profiling for aiding biomarker pattern detection and mechanistic interpretations in GC/MS based metabolomics. Metabolomics 2006; 2: 257–268
21 *Avancini G, Abreu IN, Saldana MDA, Mohamed RS, Mazzafer P.* Induction of pilocarpine formation in jaborandi leaves by salicylic acid and methyljasmonate. Phytochemistry 2003; 63: 171–175
22 *Sawaya ACHF, Abreu IN, Andreazza NL, Eberlin MN, Mazzafera P.* HPLC-ESI-MS/MS of imidazole alkaloids in *Pilocarpus microphyllus*. Molecules 2008; 13: 1518–1529
23 *Wiklund S, Johansson E, Sjostrom L, Mellerowicz EJ, Edlund U, Shockcor JP, Gottfries J, Moritz T, Trygg J.* Visualization of GC/TOF-MS-based metabolomics data for identification of biochemically interesting compounds using OPLS class models. Anal Chem 2008; 80: 115–122